

Numerical simulation on gas continuous emission from face during roadway excavation

Liang Chen^{1,2}, Enyuan Wang^{*1,2}, Junjun Feng^{1,2},
Xuelong Li^{1,2}, Xiangguo Kong^{1,2} and Zhibo Zhang^{1,2}

¹Key Laboratory of Coal Mine Gas and Fire Prevention and Control of the Ministry of Education,
China University of Mining and Technology, Xuzhou 221116, China

²School of Safety Engineering, China University of Mining and Technology, Xuzhou 221116, China

(Received October 01, 2015, Revised December 16, 2015, Accepted December 17, 2015)

Abstract. With the mining depth continuously increasing, gas emission behaviors become more and more complex. Gas emission is an important basis for choosing the method of gas drainage, gas controlling. Thus, the accurate prediction of gas emission is of great significance for coal mine. In this work, based on the sources of gas emission from the heading faces and the fluid-solid coupling process, we established a gas continuous dynamic emission model, numerically simulated and applied it to the engineering. The result was roughly consistent with the actual situation and shows the model is correct. We proposed the measures of reducing the excavation distance and borehole gas drainage based on the model. The measures were applied and the result shows the overproof problem of gas emission disappears. The model considered the influence factors of gas emission wholly, and has a wide applicability, promotional value. The research is of great significance for the controlling of gas disaster, gas drainage and pre-warning coal and gas outbursts based on gas emission anomaly at the heading face.

Keywords: gas emission; gas pressure; stress; gas drainage

1. Introduction

Gas disaster has always been considered as “the first killer” of mine safety and led to many deaths and injuries. Today, the number of gas disaster accident and its resulting casualty has been gradually declining with some pre-warning and control measures. The measures include logistic regression model, gas dilatation energy, gas content for gas outburst prediction (Xue *et al.* 2014, Li *et al.* 2015, Yu *et al.* 2015), drilling large diameter cross-measure borehole, cross-borehole hydraulic slotting technique, deep borehole blasting for gas drainage, and so on (Gao *et al.* 2015, Lin *et al.* 2015, Liu *et al.* 2015). However, the accidents have far not been completely eliminated. The important reason is that gas emission behaviors become more and more complex with the mining depth continuously increasing. Accurate prediction of gas emission is the basis for choosing the method of gas drainage, gas controlling, thus it is very important to conduct prediction research on the gas emission.

In recent years, researches on forecasting gas emission have obtained some progress. It's as

*Corresponding author, Professor, E-mail: weycumt@yeah.net

follows. Geological conditions are the important factors affecting gas emission (Saghafi *et al.* 2008). Some researchers proposed a mathematical geological method by taking into account the main geological factors of gas emission. And used historical data to forecast unmined coalbeds gas emission and achieved better results (Zhang *et al.* 2009). But the method needs lots of historical data. In general, mining companies are unwilling to provide these data as a result of company privacy.

So lots of researchers made many attempts in gas emission prediction. For example, while the forecasting model for gas emission on the heading face established by using integral method has achieved a steady-state prediction of gas emission (Guo *et al.* 2010), the gas emission model built through the source of gas emission and by introducing the inhomogeneous coefficient also realized the same goal (Li and Zhao 2011). To improve the accuracy of gas emission prediction, based on the gray model method, other methods including gray prediction model (Wei *et al.* 2011, Wu *et al.* 2014), one dimensional linear regression model (Jing *et al.* 2011), partial correlation analysis and support vector regression (SVR), as well as self-organizing data mining have also been used to predict gas emission (Li *et al.* 2014).

However, the above methods belong to the steady-state prediction. When the geological conditions changed with the mining depth increasing, it is difficult to ensure the prediction accuracy. The dynamic methods attracted researchers' attention.

For example, coupling algorithm of both chaos immune particle swarm optimization (CIPSO) and Elman neural network (ENN) (Fu *et al.* 2012), and the coupling algorithm of both colony clustering (ACC) and ENN have been proposed (Fu *et al.* 2014). However, because these methods ignored geological conditions, coalbed occurrence, their universality and accuracy still need to be further improved.

The Lunagas "Roofgas and Floorgas" geomechanical and gas emission models (Lunarzewski 1998), "the boundary element method" (Islam and Shinjo 2009), were developed to analyze gas emission or its' potential sources. However, the model built ignored the fluid-solid coupling process. It also can't achieve accurate and dynamic effect.

Gas emission is a complex fluid-solid coupling process. It involves desorption, adsorption, diffusion, etc. And gas emission is affected by geological conditions, coalbed occurrence and mining disturbance. So these factors should be considered to achieve accurate prediction.

Therefore, we will establish a gas continuous dynamic emission model considering the fluid-solid coupling process. And gas emission was numerically simulated considering geological conditions, coalbed occurrence and mining disturbance. It'll achieve accurate, dynamic and continuous prediction of gas emission finally. In addition, this study could also obviously improve the accuracy and timeliness of gas outburst early warning methods. The methods are based on gas emission, such as the early warning methods based on the gas concentration time series and based on the variation characteristics of maxima and minima of gas emission after excavating (Yang *et al.* 2010, Li and Zhou 2012).

2. Gas continuous dynamic emission model

Gas emission from coal wall is a complex process in which coalbed gas driven by the pressure gradient passes through seepage channels and into the mining space. The gas emission at the heading face is originated from coal falling, coal wall on the face, and coal walls around the roadway, respectively. Its amount can be described as follows

$$Q = Q_c + Q_f + Q_r, \quad (1)$$

Where Q is the total amount of gas emission at the heading face, m^3/min ; Q_c is the cumulative amount of gas emission from coal falling, m^3/min ; Q_f is the amount of gas emission from the coal wall of the face, m^3/min ; and Q_r is the amount of gas emission from the coal walls of the roadway, m^3/min .

Gas emission from coal walls during coal mining is continuously supplied by coal walls and controlled by underground pressure, fractures in mining-induced damaged coal mass and excavation processes. Although gas emission caused by changes in underground pressure and fractures formation has greater fluctuation in intensity during the gas decaying process, it generally obeys the exponential law (Yu *et al.* 2000). By contrast, gas from coal falling remains stable in the gas decaying process because it neither has supply source nor is controlled by underground pressure.

2.1 Amount of gas emission from coal falling

The amount of gas emission from coal falling per minute is (Yu *et al.* 2000)

$$Q_1 = Q_0 e^{-\beta_1 t_1} \quad (2)$$

where Q_1 and Q_0 are the intensity of gas emission from coal falling at time t_1 and the initial time, respectively, m^3/min ; β_1 is the decay coefficient of coal falling gas, min^{-1} ; t_1 is the retention time of coal falling at the face, min .

The amount of gas emission from coal falling as it is transported to the place with the distance L away from the heading face, Q_c , is

$$Q_c = G_c Q_0 e^{-\beta_1 t} = X S_{cs} \gamma Q_0 e^{-\beta_1 t} \quad (3)$$

where G_c is the amount of coal falling by heading, t ; X is the heading footage of the face, m ; S_{cs} is the area of roadway section, m^2 ; γ is the bulk density of coal, t/m^3 .

2.2 Amount of gas emission from the face coal wall

Given gas emission from per area of the face wall is q , $\text{m}^3/\text{m}^2 \cdot \text{min}$, i.e., the rate of gas seepage from the face coal wall, the amount of gas emission from the face wall, Q_f , is (Yu *et al.* 2000)

$$Q_f = S_{cs} q e^{-\beta_2 t_2} \quad (4)$$

where β_2 is the decaying coefficient of gas from the coal wall, min^{-1} ; t_2 is the exposure time of coal wall, min .

2.3 Amount of gas emission from the roadway coal walls

The amount of gas emission from per area of roadway coal walls is (Yu *et al.* 2000)

$$Q_3 = qe^{-\beta_2 t_2} \quad (5)$$

where Q_3 is the amount of gas emission from per area of roadway coal walls at time t_2 , $\text{m}^3/\text{m}^2 \cdot \text{min}$.

Let dL represents a small length along the coal walls and the amount of gas emission from roadway around dL obeys Eq. (5), the amount of gas emission at time t_2 is

$$dQ_3 = qe^{-\beta_2 t_2} Adl \quad (6)$$

where A is the area of the roadway wall, m^2 .

After advancing X meters, from the heading face to the place at a distance L away from the heading face, the amount of gas emission from the roadway coal walls, Q_r , is the integral of Eq. (6), that is

$$Q_r = q \int_0^{L+X} e^{-\beta_2 t_2} Adl = qA(L+X)e^{-\beta_2 t_2} \quad (7)$$

2.4 Model for gas emission from coal wall

In order to study the characteristics of gas emission from coal wall, we assumed that: (1) the process of coalbed gas migration is an isothermal process; (2) free gas is the ideal gas obeying the equation of state of ideal gas; (3) the coal is the medium of continuity; (4) the elastoplastic transformation of the gas-bearing coal is small enough; and (5) the flow of gas in the coal is unidirectional and unsteady (Palmer 2009, Liu and Rutqvist 2010, Qin *et al.* 2015).

Gas adsorption obeys the Langmuir equation and gas content is expressed as

$$X_m = \frac{abp}{1+bp} + Bnp \quad (8)$$

Where X_m is the content of gas per unit mass of coal, m^3/t ; a is the limit adsorption amount of coal, m^3/t ; b is the adsorption equilibrium constant, MPa^{-1} ; p is the pressure of coalbed gas, MPa ; n is the porosity of coal; $B = T_0/(Tp_0\zeta\rho)$ is the coefficient, $\text{m}^3/(\text{t}\cdot\text{MPa})$, T_0 is the absolute temperature under standard conditions, $T_0 = 273 \text{ K}$; T is gas temperature, K ; p_0 is the atmospheric pressure under standard conditions; $p_0 = 0.101325 \text{ MPa}$; ζ is the compression coefficient of gas; and ρ is the apparent density of coal, t/m^3 .

The process of gas flow in the coalbed satisfies the Darcy's law

$$u = -\frac{k}{\mu} \frac{\partial p}{\partial x} \quad (9)$$

where u is the velocity of gas flow, m/s ; k is the permeability of coalbed, m^2 ; μ is the dynamic viscosity of gas, $\text{MPa}\cdot\text{s}$; and $\partial p/\partial x$ is the gradient of gas pressure, MPa/m . Applying the equation of state of ideal gas to convert the amount of gas emission from per area of coal wall to the volume flow rate at the standard atmospheric pressure finds Eq. (9) is changed as follows

$$\frac{q}{1440} = -\frac{k}{2\mu p_0} \frac{\partial p^2}{\partial x} \quad (10)$$

According to the law of conservation of mass, the mathematical model for gas emission from coal wall is

$$\frac{\partial p}{\partial t_2} = \frac{pk}{\rho[\frac{ab}{(1+bp)^2} + Bn]\mu p_0} \frac{\partial^2 p^2}{\partial x^2} \tag{11}$$

2.5 Mathematical model for gas continuous dynamic emission

Jointly solving Eqs. (1), (3), (4), (7), (10) and (11) can find the mathematical model for gas emission from the heading face as follows

$$\begin{cases} Q = XS_{cs}\gamma Q_0 e^{-\beta t_1} + [S_{cs} e^{-\beta t_2} + A(L+X)e^{-\beta t_2}](-\frac{720k}{\mu p_0} \frac{\partial p^2}{\partial x}) \\ \frac{\partial p}{\partial t_2} = \frac{pk}{\rho[\frac{ab}{(1+bp)^2} + Bn]\mu p_0} \frac{\partial^2 p^2}{\partial x^2} \end{cases} \tag{12}$$

The mathematical model for gas emission is a complex nonlinear partial differential equations system. It is necessary to introduce the permeability model (Perera *et al.* 2013, Guo *et al.* 2014).

$$\frac{k}{k_0} = \left\{ 1 - \frac{\alpha}{\varphi_0 K} [(\bar{\sigma} - \bar{\sigma}_0) - (p_1 - p)] - \frac{f_m}{\varphi_0} \left(\frac{\varepsilon_{\max} p_1}{p_1 + p_L} - \frac{\varepsilon_{\max} p}{p + p_L} \right) \right\}^3 \tag{13}$$

where k_0 is the initial permeability and porosity of coalbed, m^2 ; φ_0 is the initial porosity of coalbed; α is Biot's coefficient; K is the bulk modulus of coal, MPa; $\bar{\sigma}$ is the mean stress, MPa; $\bar{\sigma}_0$ is the origin stress, MPa; p_1 is the gas pressure, MPa; f_m is effective coal matrix deformation factor between 0 and 1 for a particular coal; ε_{\max} is the maximum adsorption strain when the gas pressure is infinite; p_L is called the Langmuir pressure and defined as the pressure when the adsorption strain is half of the maximum adsorption strain, MPa.

Putting Eq. (12) into Eq. (13) finds, gas continuous dynamic emission can be written as

$$\begin{cases} \frac{\partial p^2}{\partial x} = \frac{-\mu p_0 (Q - XS_{cs}\gamma Q_0 e^{-\beta t_1})}{720k_0 [S_{cs} e^{-\beta t_2} + A(L+X)e^{-\beta t_2}] \left\{ 1 - \frac{\alpha}{\varphi_0 K} [(\bar{\sigma} - \bar{\sigma}_0) - (p_1 - p)] - \frac{f_m}{\varphi_0} \left(\frac{\varepsilon_{\max} p_1}{p_1 + p_L} - \frac{\varepsilon_{\max} p}{p + p_L} \right) \right\}^3} \\ \frac{\partial^2 p^2}{\partial x^2} = \frac{\rho[\frac{ab}{(1+bp)^2} + Bn]\mu p_0}{pk_0 \left\{ 1 - \frac{\alpha}{\varphi_0 K} [(\bar{\sigma} - \bar{\sigma}_0) - (p_1 - p)] - \frac{f_m}{\varphi_0} \left(\frac{\varepsilon_{\max} p_1}{p_1 + p_L} - \frac{\varepsilon_{\max} p}{p + p_L} \right) \right\}^3} \frac{\partial p}{\partial t_2} \end{cases} \tag{14}$$

with its initial and boundary conditions

$$\begin{cases} p(x,t)|_{t=0} = p_1 (0 < x \leq l) \\ p(x,t)|_{x=0} = p_0 (t > 0) \\ \left. \frac{\partial p}{\partial l} \right|_{x=l} = 0 (t > 0) \end{cases} \quad (15)$$

where l is the impacting region of gas flow, m .

The model considered the sources of gas emission, the fluid-solid coupling process. It also can be seen that the model is a complex nonlinear partial differential equation.

3. Geological background and model parameters

Gas continuous dynamic emission model is a nonlinear partial differential equation. It's difficult to solve the value directly. So we can use Comsol Multiphysics to convert a multiple physics field coupling mathematical model into a unified system of partial differential equations, and calculate gas emission. In addition, geological conditions, coalbed occurrence and mining disturbance can be considered, too.

3.1 Geological background

Jiulishan Coal Mine, Henan Energy and Chemical Industry Group Co. Ltd., is located in Jiaozuo City, Henan Province, China, as shown in Fig. 1. It was built in 1970, with its design capacity of 0.9 Mt/a. It is typical coal and gas outburst mine. In history occurred 64 coal and gas outburst accidents, among which 53 occurred at the heading faces, and 37 were induced by excavation, accounting for 69.8% of coal and gas outburst accidents at the heading faces. In the production process, gas emission exceeds its limit and significantly affected its production.

Gas concentration isn't allowed to exceed 1% by the State Administration of Coal Mine Safety. For safety production, the limit of gas concentration at heading face was set at 0.8% by Henan Energy and Chemical Industry Group Co. Ltd. So it caused more serious gas emission overrun problem. Some heading faces had to stop mining for months, seriously affecting the mining and excavating.

No. 14141 Face of Jiulishan Coal Mine had burying depth of about 480 m, design roadway width of 4m, height of 3 m and thickness of coal bed of 2.8~3.1 m with average of 3 m, coalbed dip angle of 12°, Protodyakonov's coefficient of 0.25, initial velocity of gas emission Δp of 18~30, the content and pressure of gas in coalbed of 19.17m³/t and 1.74 MPa, respectively. The air volume at the face was 540 m³/min, the over-limit of gas concentration was exchanged into the amount of gas emission of 4.32 m³/min. Before excavation, some regional coal and gas outburst prevention measures were taken, including gas pre-drainage from sublevel coalbed and subsection roadway through bedding drilling; and advance gas emission through local drilling as local coal and gas outburst prevention measures.

The gas pressure of roadway from excavation to 120 m footage was 0.28~0.32 MPa. To reduce gas pressure, A total of 20~30 boreholes were drilled and gas was naturally drained for 8~12 hours. Afterwards, no gas emission overrun accident occurred. When the heading footage reached 120 m,



Fig. 1 Location of the area under study

the gas pressure of coal seam was up to 0.36 MPa; after a continuous heading of 1.2 m, the gas emission reached 4.62 m³/min, the heading had to be stopped due to the above-limit.

3.2 Model parameters

With the geological conditions of No. 14141 Face at its heading footage of 120 m as the model prototype, both the length and width of the model were 50 m, and its height was 14 m, among which the roof thickness was 6 m, the floor thickness 5 m, and the coal thickness 3 m. Its bottom was fixed with constraint, while its laterals were capable of horizontal displacement. To make the simulation results to better meet the actual situation, the model performed stepwise mining. The first step was to mine the dark blue coal body, as shown in Fig. 2. After excavation, the mechanical

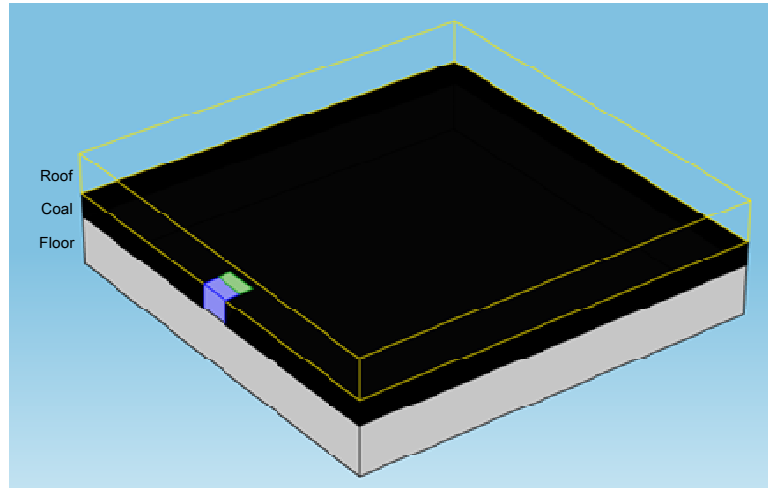


Fig. 2 Schematic of geometrical model

process of gas-bearing coal was numerically computed to find the stress-strain field after coal and rock mining. After natural emission, the second step excavation started according to the driving footage. The excavation section was shown by the fluorescent green in Fig. 2.

Gas flow only occurred in the coalbed, and the gas pressure to the coal walls was equal to the atmospheric pressure. Table 1 lists the initial physical parameters chosen by the geometrical model.

Table 1 Basic physical parameters of the geometrical model

Parameter	Value
Elastic modulus of roof and floor rocks	30000 MPa
Poisson's ratio of roof and floor rocks	0.22
Density of roof and floor rocks	2.5 t/m ³
Cohesive force of roof and floor rocks	40 MPa
Internal friction angle of roof and floor rocks	34°
Elastic modulus of coal	2600 MPa
Poisson's ratio of coal	0.22
Cohesive force of coal	2.1 MPa
Internal friction angle of coal	30°
Biot's coefficient	0.9
Pressure of coalbed gas	0.36 MPa
Limit adsorption amount of coal	30.7 m ³ /t
Adsorption equilibrium constant	0.4 MPa ⁻¹
Gas temperature	293 K
Compression coefficient of gas	1.07
Effective coal matrix deformation factor	0.1
Langmuir pressure	1.2 MPa

Table 1 Continued

Parameter	Value
Initial porosity of coalbed	0.046
Initial permeability of coalbed	$1.5 \times 10^{-15} \text{ m}^2$
Dynamic viscosity coefficient of gas	$1.84 \times 10^{-5} \text{ Pa}\cdot\text{s}$
Density of gas	0.717 kg/m^3
Atmospheric pressure at the face	0.1 MPa
Area of roadway cross section	12 m^2
Bulk density of coal	1.4 t/m^3
Intensity of gas emission from initial coal falling	$0.182 \text{ m}^3/\text{t}\cdot\text{min}$
Decaying coefficient of coal falling gas	0.098 min^{-1}
Decaying coefficient of coal wall gas	0.0061 min^{-1}

4. Numerical simulation verification

Fig. 3 shows the simulated results of gas emission from No.14141 Face after excavating for 1.2 m from its 120 m footage geological condition model. From the figure it is clear that the error between simulated result of gas emission at the moment after excavation and the actual gas emission value was 5.41%. The error at 65 minutes after excavation was the maximum, 18.2%, which may be result in shoveling coal by miners. According to the Jiulishan Coal Mine’s rule, it’s not allowed to do anything after excavation 45 minutes. It’s to avoid gas accident. Simulation results were roughly consistent with the actual situation. It indicated that the gas emission model was correct.

After excavation, gas emission from the face was characteristic of a first rapid then very slow reduction trend over time, which is closely related to the spatiotemporal evolution behaviors of both stress and gas process. Figs. 4 and 5 show the spatiotemporal evolution behaviors of both stress and gas process at the face, among these figures, Figs. (a) and (b) in Figs. 4 and 5 show

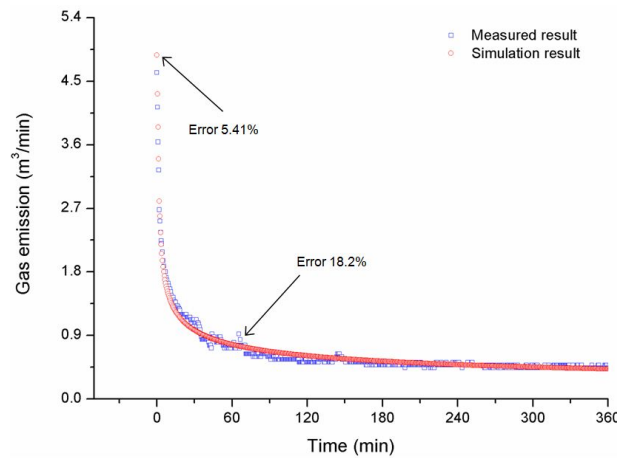


Fig. 3 Simulated result of gas emission after excavation

the spatiotemporal evolution behaviors of both stress and gas process in the front of the working face and its bilateral at the center of the head-on coal wall, respectively.

It can be seen from Fig. 4 that under the impact of excavation at the face, the maximum stress in the front of the working face was 37.04 MPa at about 2.5 m away from the face. At 30 min after excavation, the maximum stress in the front of the working face was 33.9 MPa at about 2.7 m away from the face, indicating that the stress peak decreased rapidly and moved backward. At 180 min, the stress peak dropped to 32.3 MPa, at approximately 2.8 m away from the face. Over time, the decline in stress peak became slower. The peak at 360 min was slight smaller than that at 180 min. The spatiotemporal evolution of stress at both sides of the face was roughly consistent with that of stress in the front of the working face; the differences between them were that the stress concentration values of both sides were slightly smaller than those of the front of the working face at the excavating moments of 30, 180 and 360 min. Thus, no matter where in the front of the working face or its bilateral, after excavation, the stress peaks all dropped and moved gradually far away from the face.

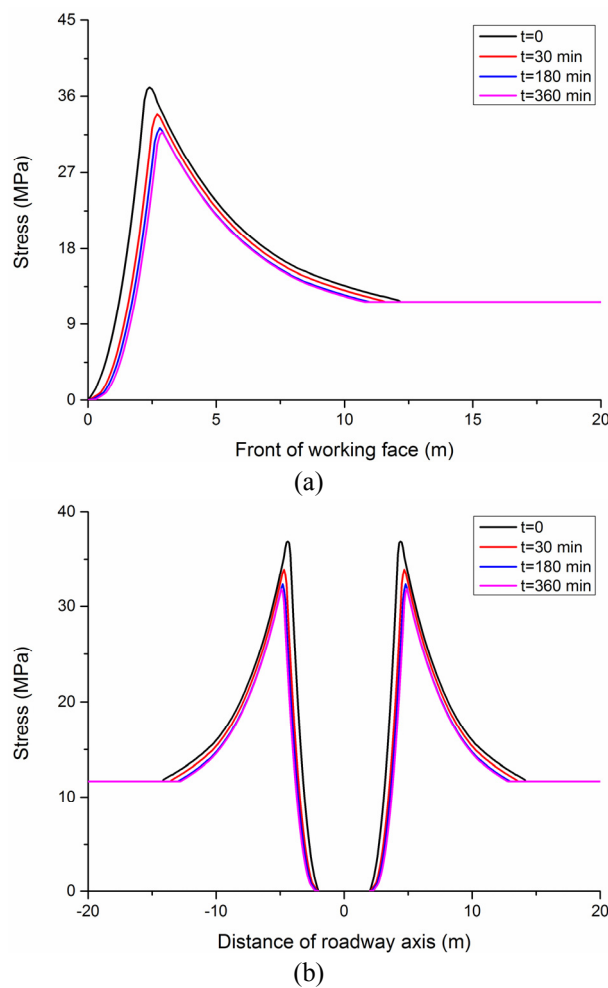


Fig. 4 Spatiotemporal evolution of stress at (a) front of the working face; and (b) bilaterals of the face

From Fig. 5 it is clear that at the excavation moments, 30, 180 and 360 min, the distances of the gas pressure increasing from the atmospheric pressure to the initial gas pressure in order were 8.4, 8.6, 8.7 and 8.8 m, while the gradients of gas pressure in order were 0.031, 0.0302, 0.0299 and 0.0295 MPa/m. Thus, over time, the gradient of gas pressure gradually decreased. The spatiotemporal evolution of gas pressure in both sides of the face were roughly consistent with that of gas pressure in the front of the working face; the differences between them were that the distances of gas pressure increasing from the atmospheric pressure to the initial gas pressure became farther and farther. Thus, no matter where in the front of the working face or its both sides, after coal excavation, the gradient of gas pressure all dropped.

The evolution of stress and gas pressure directly affected gas emission from the face after excavation, especially, at the excavation instant. Roadway excavation caused sudden stress relief of coal, which further affected coal in the front of the working face, leading to a sudden rise in stress with its stress peak closer to the working face. Cracks propagated in the coal, which opens gas flow channels, suddenly enlarges gas pressure gradient meantime and speeds up gas flow. This

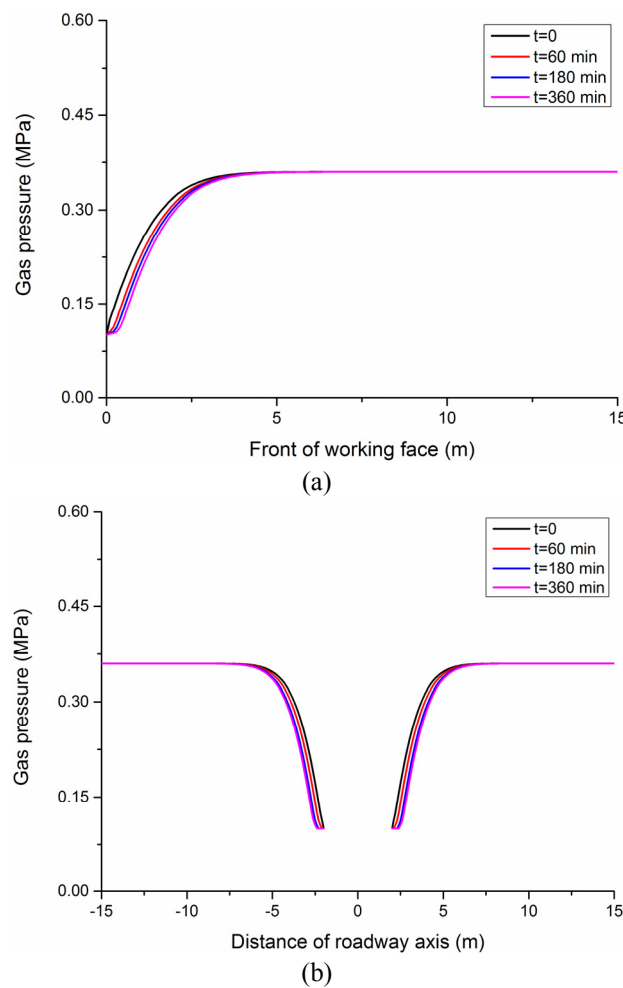


Fig. 5 Spatiotemporal evolution of gas pressure at (a) front of the working face; and (b) bilaterals of the face

is also the cause for rapid increase of gas emission at the excavation instant. Wang *et al.*, in their seepage tests and CT scan tests in the whole stress-strain process, found that before the seepage experiment, roughly no micropores or cracks in the coal were observed (Wang *et al.* 2012); while after the experiment, evident micropores or cracks were monitored. Ou *et al.* in their laboratory found and confirmed that the greater the stress and gas pressure are, the more serious the degree of its breaking, and the more the cracks develop (Ou *et al.* 2012). Both researches proved that at the moment after excavation, increase in gas emission is closely related to stress and gas pressure.

Because stress rapidly transfers to the deep, coal pores and cracks are gradually compacted, the seepage of gas in the deep coal toward the face becomes more and more difficult. With rapid decline in gas pressure gradient, gas amount in the face coal also lowers rapidly after excavation. With the time further advancing, coal pores and cracks expand slowly and passages of gas flow gradually stabilizes, and decline in gas pressure gradient results in the slow reduction in gas emission from the face. After excavation, the characteristics of gas emission from the face reflect the spatiotemporal variability of stress and gas pressure. The increase in gas emission from the face at the instant after excavation is resulted from rapid enhancement in stress and gas pressure gradient.

5. Engineering application

According to analyses of geological conditions, coalbed occurrence, disturbance, and other factors of No.14141 Heading Face of Jiulishan Coal Mine, the main factors impacting gas emission overrun are gas pressure and mining disturbance. A total of 20~30 boreholes were drilled on the face and the natural emission was implemented for 8~12 hours to reduce gas pressure. However, because the coalbed was soft and prone to drilling collapse in production, it was difficult by increasing the number of boreholes to lower gas pressure. Therefore, to seek new methods to avoid gas emission overrun, the effects of both gas drainage time and excavating footage on gas emission were analyzed.

5.1 Effect of gas drainage time on gas emission

Reducing coal seam gas pressure is the main solution to gas emission overrun. A proper delay of the gas drainage time was beneficial to decline in gas pressure. In this study, gas emission after drainage time of 12, 48, 96 and 144 h was analyzed. Figs. 6 and 7 shows the distribution characteristics of stress and gas pressure, respectively, after gas drainage time of 12, 48, 96, and 144 h. Fig. 8 shows the numerical simulation results of gas emission at different gas drainage time.

From Fig. 6, it is clear that after gas drainage time of 12, 48, 96 and 144 h, the stress peaked at 37.04, 36.8, 36.4 and 36.3 MPa, respectively. And the stress peaks were 2.5, 2.6, 2.6 and 2.6 m in front of working face, respectively. With the drainage time prolonging, it seemed the reduction in stress was not obvious.

From Fig. 7, it is clear that the distance of gas pressure increasing from the atmospheric pressure to the initial gas pressure at the gas drainage time of 12, 48, 96 and 144 h was 8.4, 8.51, 8.55 and 8.59 m and the gas pressure gradient was 0.031, 0.0306, 0.0304 and 0.0303 MPa/m, respectively. With the drainage time prolonging, the gradient of gas pressure decreased a little.

From Fig. 8, it is clear that the maximum amount of gas emission was 4.87, 4.58, 4.38 and 4.29 m³/min at gas drainage time of 12, 48, 96 and 144 h, respectively. With the drainage time

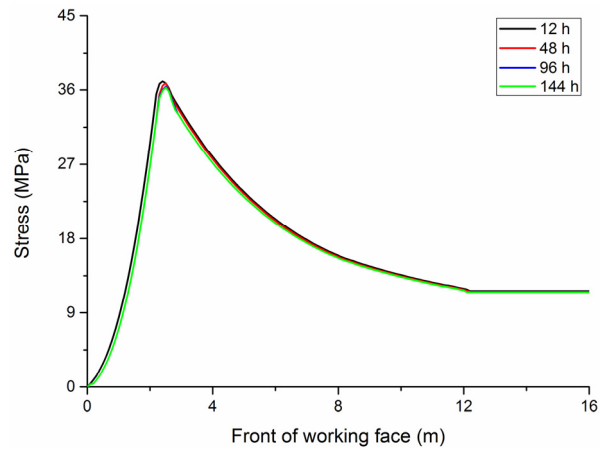


Fig. 6 Distribution of stress on the face at different gas drainage time

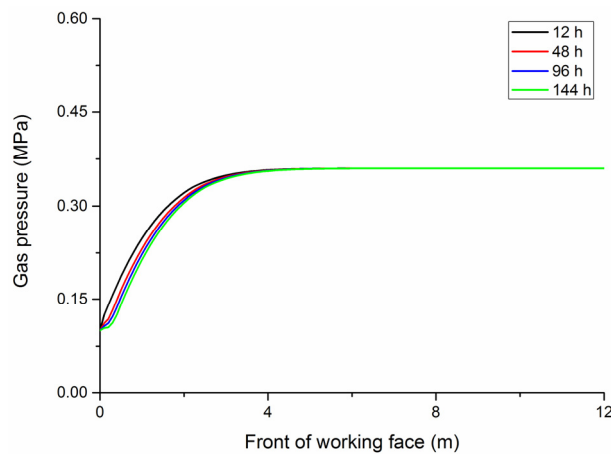


Fig. 7 Distribution of gas pressure on the face at different gas drainage time

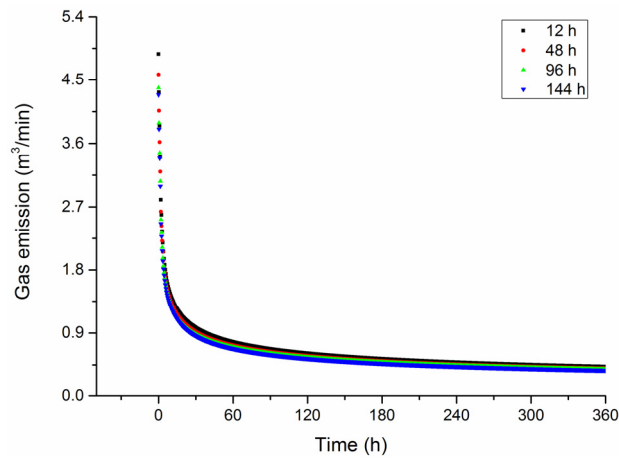


Fig. 8 Characteristics of gas emission from the face at different gas drainage time

prolonging, gas emission decreased. It can explain from the effects of gas on the coal mechanic behaviors. On the one hand, the pores and cracks in high gas-containing coal more easily generate and expand; on the other hand, high gas-containing coal is easily failure (Wang *et al.* 2014). Thus, prolonging gas drainage time to reduce gas pressure on coalbed cannot only avoid the formation of a higher gas flow, but also increase coal strength. The method can reduce gas emission.

5.2 Effect of footage on gas emission

Roadway excavation is the direct cause for a sharp increase in gas emission from the face. Figs. 9 and 10 show the characteristics of stress and gas pressure on the face at the instant after roadway excavation, respectively, at the heading footage of 0.6, 0.9, 1.2 and 1.5 m. Fig. 11 shows the numerically simulated results of gas emission at different heading footage after excavation.

It can be seen from Fig.9 that when coal excavation advanced to 0.6, 0.9, 1.2 and 1.5 m, the corresponding stress peak was 30.00, 33.34, 37.04 and 40.74 MPa at 3.1, 2.7, 2.5 and 2.3 m,

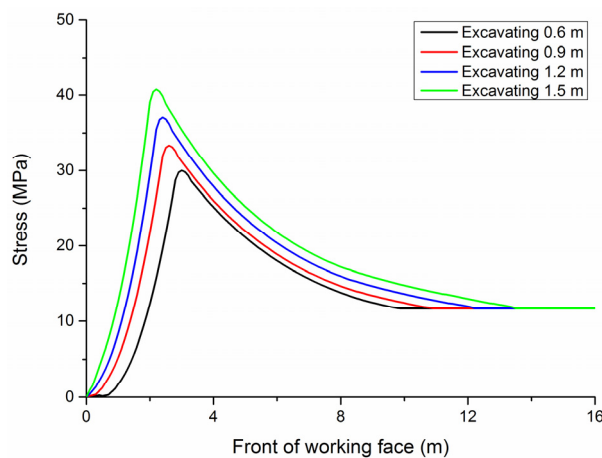


Fig. 9 Distribution of stress on the face at different heading footage

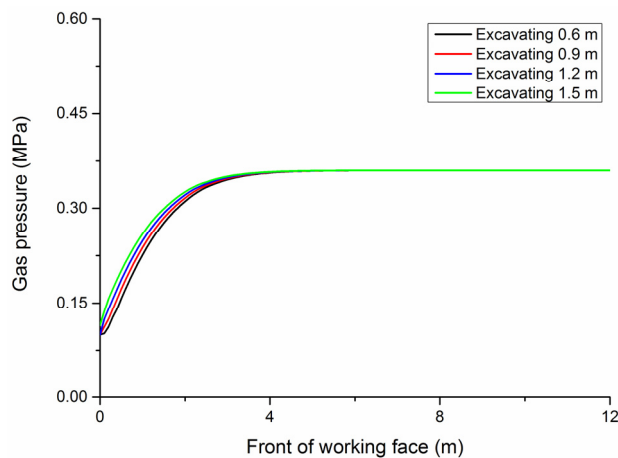


Fig. 10 Distribution of gas pressure on the face at different heading footage

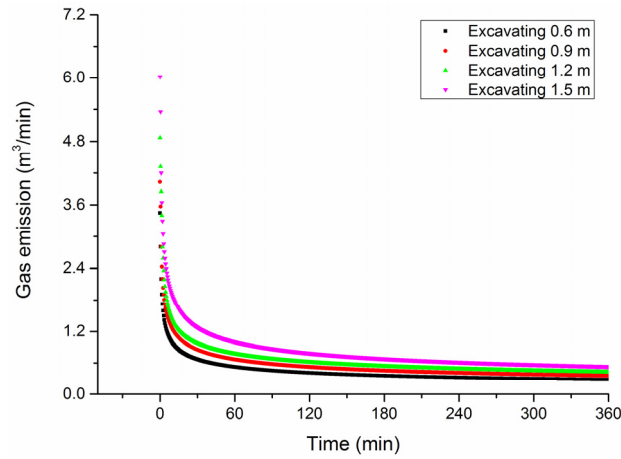


Fig. 11 Characteristics of gas emission from the face at different heading footage

respectively, away from the face and the resultant stress gradient was 9.68, 12.35, 14.82 and 17.71 MPa/m, respectively. Among them, the gradient of stress at the excavation footage of 1.5 m was up to 1.83 times of that at the excavation footage of 0.6 m. With the excavation footage increasing, the stress concentration value became more obvious and the resultant stress gradient was greater.

It can be seen from Fig. 10 that when coal excavation advanced to 0.6, 0.9, 1.2 and 1.5 m, respectively, the distance of the gas pressure rising from the atmospheric pressure to the initial gas pressure was 9.04, 8.78, 8.4 and 8.14 m, respectively and the corresponding gas pressure gradient was 0.0288, 0.0296, 0.031 and 0.032 MPa/m, respectively, indicating that gas pressure gradient increases significantly.

It can be seen from Fig. 11 that more gas was emitted at greater excavated footage. The maximum gas emission at the excavated footage 0.6, 0.9, 1.2 and 1.5 m were 3.45, 4.03, 4.87 and 6.02 m³/min, respectively.

On the one hand, with the excavation footage increasing, the amount of coal falling increased. For every 50% increase in driving footage, the amount of coal falling and gas emission increased by 50%; On the other hand, with the excavation footage increasing, (1) the excavated high stress area was closer to the face; (2) the coal in this area was more prone to cracking and forming more developed crack channels; and (3) the gas pressure gradient was greater, all these were in favor to gas emission. Therefore, increase in excavation footage significantly affects the distributions of stress and gas pressure and is in favor to gas emission.

5.3 Application effect

According to the simulation results, after 144 h of gas drainage through boreholes, gas emission after excavation wouldn't overrun. And after excavation advanced 0.6 and 0.9 m, the maximum gas emission reached 3.45 and 4.03 m³/min, respectively. Thus, reducing gas emission by extending drainage time needs more time, while reducing gas emission by shortening excavating distance could achieve better effect. Therefore, to ensure safety production, both excavating 0.6 m and local gas drainage through boreholes should be adopted in Jiulishan Coal Mine.

Fig. 12 shows the maximum gas emission after the remaining footage excavated using two

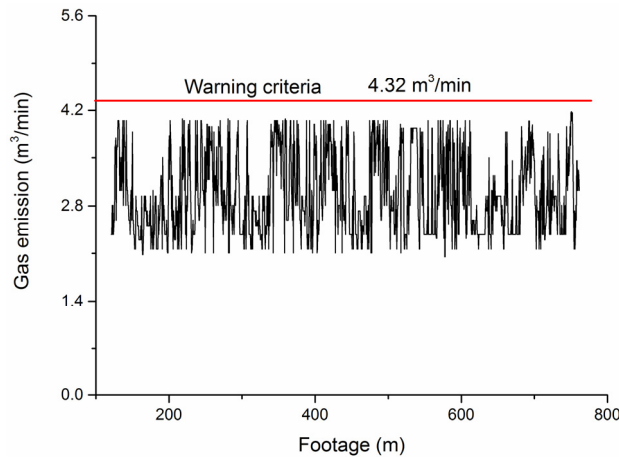


Fig. 12 The maximum gas emission to footage in between 121~761 m

measures. It can be seen from the figure that no gas emission overrun occurred. The gas continuous dynamic emission model's value is of great and worth of widely using.

6. Conclusions

The paper focused on the study of gas emission during the roadway excavation. The conclusions are as follows:

- (1) We established a gas continuous dynamic emission model considering the fluid-solid coupling process, and numerically simulated gas emission. The simulated results of gas emission from the face after excavation were roughly consistent with the actual situation.
- (2) The characteristics of gas emission from the face reflect the spatiotemporal variability of stress and gas pressure after excavation. The increase in gas emission from the face after excavation is resulted from rapid enhancement in stress and gas pressure gradient.
- (3) According to analyses of gas emission impacting factors with the model, we proposed measures of reducing excavation distance along with local gas drainage through boreholes to solve face gas emission overrun.

We believe this study is significance to enhance gas disaster prevention, gas drainage and control ability and improve coal and gas outburst early-warning techniques.

Acknowledgments

This work is supported by the Research Project of Chinese Ministry of Education (No.113031A), the Outstanding Innovative Team of China University of Mining and Technology (No. 2014ZY001), and the Priority Academic Program Development of Jiangsu Higher Education Institutions (PAPD). The authors acknowledge the contributions of Jiulishan Coal Mine for providing access to the data. The authors also acknowledge Miss Anne for improving the language in this paper.

References

- Fu, H., Jiang, W. and Shan, X. (2012), "Study on coupling algorithm on coal mine gas emission forecast model", *J. China Coal Soc.*, **37**(4), 654-658.
- Fu, H., Xie, S., Xu, Y. and Chen, Z. (2014), "Gas emission dynamic prediction model of coal mine based on ACC-ENN algorithm", *J. China Coal Soc.*, **39**(7), 1296-1301.
- Guo, X., Cai, W., Ma, S., Jiang, Z. and Chen, X. (2010), "Continuity prediction of gas emission during drive in coal seam based on stable percolation", *J. China Coal Soc.*, **35**(6), 932-936.
- Guo, P., Cheng, Y., Jin, K., Li, W., Tu, Q. and Liu, H. (2014), "Impact of effective stress and matrix deformation on the coal fracture permeability", *Transport in Porous Media*, **103**(1), 99-115.
- Gao, Y., Lin, B., Yang, W., Li, Z., Pang, Y. and Li, H. (2015), "Drilling large diameter cross-measure boreholes to improve gas drainage in highly gassy soft coal seams", *J. Natural Gas Sci. Eng.*, **26**, 193-204.
- Islam, M.R. and Shinjo, R. (2009), "Numerical simulation of stress distributions and displacements around an entry roadway with igneous intrusion and potential sources of seam gas emission of the Barapukuria coal mine, NW Bangladesh", *Int. J. Coal Geol.*, **78**(4), 249-262.
- Jing, G., Xu, S., Heng, X. and Li, C. (2011), "Research on the prediction of gas emission quantity in coal mine based on grey system and linear regression for one element", *Procedia Engineering*, **26**, 1585-1590.
- Li, Y. and Zhao, D. (2011), "Prediction study on gas emission of the first face in the 11-2 coal seam in Liuzhuang Coal Mine", *Procedia Engineering*, **26**, 883-889.
- Li, X. and Zhou, W. (2012), "The risk forecast of coal and gas outburst on blasting-working face by the method of gas peak-to-valley ratio", *J. China Coal Soc.*, **37**(S1), 104-108.
- Li, R., Shi, S., Wu, A., Luo, W. and Zhu, H. (2014), "Research on prediction of gas emission based on self-organizing data mining in coal mines", *Procedia Engineering*, **84**, 779-785.
- Li, Z., Wang, E., Ou, J. and Liu, Z. (2015), "Hazard evaluation of coal and gas outbursts in a coal-mine roadway based on logistic regression model", *Int. J. Rock Mech. Min. Sci.*, **80**, 185-195.
- Lin, B., Yan, F., Zhu, C., Zhou, Y., Zou, Q., Guo, C. and Liu, T. (2015), "Cross-borehole hydraulic slotting technique for preventing and controlling coal and gas outbursts during coal roadway excavation", *J. Natural Gas Sci. Eng.*, **26**, 518-525.
- Liu, H. and Rutqvist, J. (2010), "A new coal-permeability model: Internal swelling stress and fracture – matrix interaction", *Transport in Porous Media*, **82**(1), 157-171.
- Liu, J., Liu, Z., Xue, J., Gao, K. and Zhou, W. (2015), "Application of deep borehole blasting on fully mechanized hard top-coal pre-splitting and gas extraction in the special thick seam", *Int. J. Min. Sci. Technol.*, **25**(5), 755-760.
- Lunarzewski, L.L.W. (1998), "Gas emission prediction and recovery in underground coal mines", *Int. J. Coal Geol.*, **35**(1), 117-145.
- Ou, J., Wang, E., Ma, G., Wang, C., Song, D., Chen, P. and Li, N. (2012), "Coal rupture evolution law of coal and gas outburst process", *J. China Coal Soc.*, **37**(6), 978-983.
- Palmer, I. (2009), "Permeability changes in coal: Analytical modeling", *Int. J. Coal Geol.*, **77**(1-2), 119-126.
- Perera, M.S.A., Ranjith, P.G. and Choi, S.K. (2013), "Coal cleat permeability for gas movement under triaxial, non-zero lateral strain condition: A theoretical and experimental study", *Fuel*, **109**, 389-399.
- Qin, Y., Liu, P., Hao, Y., Wang, J. and Wu, J. (2015), "Mathematical model of gas emission of coal wall and its numerical analysis", *J. Liaoning Tech. Univ.*, **34**(10), 1105-1110.
- Saghafi, A., Pinetown, K.L., Grobler, P.G. and van Heerden, J.H.P. (2008), "CO₂ storage potential of South African coals and gas entrapment enhancement due to igneous intrusions", *Int. J. Coal Geol.*, **73**(1), 74-87.
- Wang, G., Xue, D., Gao, H. and Zhou, H. (2012), "Study on permeability characteristics of coal rock in complete stress-strain process", *J. China Coal Soc.*, **37**(1), 107-112.
- Wang, T., Wang, Z., Liu, H., Guan, Y. and Zhan, S. (2014), "Discussion about the mechanism of gas disaster induced by coal bump", *J. China Coal Soc.*, **39**(2), 371-376.
- Wei, C., Xu, M., Sun, J., Li, X. and Ji, C. (2011), "Coal mine gas emission gray dynamic prediction", *Procedia Engineering*, **26**, 1157-1167.
- Wu, L., Liu, S., Chen, D., Yao, L. and Cui, W. (2014), "Using gray model with fractional order

- accumulation to predict gas emission”, *Natural Hazards*, **71**(3), 2231-2236.
- Xue, S., Yuan, L., Xie, J. and Wang, Y. (2014), “Advances in gas content based on outburst control technology in Huainan, China”, *Int. J. Min. Sci. Technol.*, **24**(3), 385-389.
- Yang, S., Tang, J., Zhao, S. and Hua, F. (2010), “Early Warning on Coal and Gas Outburst with Dynamic Indexes of Gas Emission”, *Disaster Advances*, **3**(4), 403-406.
- Yu, Q., Wang, K. and Yang, S. (2000), “Study on pattern and control of gas emission at coal face in China”, *J. China Univ. Min. Technol.*, **29**(1), 9-14.
- Yu, B., Su, C. and Wang, D. (2015), “Study of the features of outburst caused by rock cross-cut coal uncovering and the law of gas dilatation energy release”, *Int. J. Min. Sci. Technol.*, **25**(3), 453-458.
- Zhang, X., Shan, J. and Peng, S. (2009), “Mathematical geology technique and method for prediction of gas content and emission”, *J. China Coal Soc.*, **34**(3), 350-354.

CC